LHCb-CONF-2011-001
March 25, 2011
Version 4.0

b-hadron lifetime measurements with exclusive $b \to J/\psi X$ decays reconstructed in the 2010 data

The LHCb Collaboration[1]

Abstract

We report on absolute lifetime measurements in the exclusive decays $B^+ \to J/\psi K^+$, $B^0 \to J/\psi K^{*0}$, $B^0 \to J/\psi K^0_S$, $B^0_s \to J/\psi \phi$ and $\Lambda_b \to J/\psi \Lambda$ using $36\,\text{pb}^{-1}$ of data collected in 2010 with the LHCb detector and a muon trigger at a centre-of-mass energy of 7 TeV. From a maximum likelihood fit to the proper time distribution of fully reconstructed candidates in each decay mode, we measure

$$\begin{aligned}
\tau(B^+ \to J/\psi K^+) &= 1.689 \pm 0.022\ (\text{stat.}) \pm 0.047\ (\text{syst.})\ \text{ps}\,, \\
\tau(B^0 \to J/\psi K^{*0}) &= 1.512 \pm 0.032\ (\text{stat.}) \pm 0.042\ (\text{syst.})\ \text{ps}\,, \\
\tau(B^0 \to J/\psi K^0_S) &= 1.558 \pm 0.056\ (\text{stat.}) \pm 0.022\ (\text{syst.})\ \text{ps}\,, \\
\tau^{\text{single}}(B^0_s \to J/\psi \phi) &= 1.447 \pm 0.064\ (\text{stat.}) \pm 0.056\ (\text{syst.})\ \text{ps}\,, \\
\tau(\Lambda_b \to J/\psi \Lambda) &= 1.353 \pm 0.108\ (\text{stat.}) \pm 0.035\ (\text{syst.})\ \text{ps}\,,
\end{aligned}$$

where $\tau^{\text{single}}(B^0_s \to J/\psi \phi)$ is the lifetime measured with $B^0_s \to J/\psi \phi$ using a single exponential to model the proper time distribution, i.e., ignoring the non-zero decay-width difference of the B^0_s system.

[1]Conference note prepared for the 2011 Winter Conferences; contact authors: Greig Cowan (greig.cowan@cern.ch) and Yuehong Xie (yuehong.xie@cern.ch).

1 Introduction

Exclusive $b \to J/\psi X$ decays allow the pursuit of several important measurements at LHCb. $B_s^0 \to J/\psi\phi$ is the golden decay channel to probe new physics in B_s^0 mixing by measuring the CP-violating phase ϕ_s induced by interference between decay amplitudes with and without B_s^0 mixing and measuring the decay width difference of the B_s^0 system, $\Delta\Gamma_s = \Gamma_{s,L} - \Gamma_{s,H}$, where $\Gamma_{s,L}$ and $\Gamma_{s,H}$ refer to the decay widths of the light and heavy eigenstates, respectively. These measurements require a good understanding of detector effects such as the proper time acceptance and resolution, angular acceptance, mistag fraction and background. The strategy presented here is to trigger and select several $b \to J/\psi X$ decay modes in a similar way and use them as control channels to calibrate the detector and validate the analysis procedures used when studying $B_s^0 \to J/\psi\phi$.

The B^+ and B^0 lifetimes have been measured to a high precision in other experiments, as seen in Table 1. Therefore, measurements of b-hadron lifetimes at LHCb provide an ideal testbed for LHCb's capacity to perform time-dependent analyses. In this conference note we report on measurements of the lifetime of b-hadron species with the decays $B^+ \to J/\psi K^+$, $B^0 \to J/\psi K^{*0}$, $B_s^0 \to J/\psi\phi$, $B^0 \to J/\psi K_S^0$ and $\Lambda_b \to J/\psi\Lambda$ followed by $J/\psi \to \mu^+\mu^-$.

b-hadron lifetime	PDG evaluation (ps)
τ_{B^+}	1.638 ± 0.011
τ_{B^0}	1.525 ± 0.009
$\tau_{B_s^0}$	$1.472^{+0.024}_{-0.026}$
τ_{Λ_b}	$1.391^{+0.038}_{-0.037}$

Table 1: PDG evaluations of the b-hadron lifetimes [1]. The quoted B_s^0 lifetime is $1/\Gamma_s$ where $\Gamma_s = (\Gamma_{s,\mathrm{L}} + \Gamma_{s,\mathrm{H}})/2$.

2 Data sample and event selection

We use a data sample corresponding to an integrated luminosity of approximately $36\,\mathrm{pb}^{-1}$ collected with the LHCb detector in 2010 in proton-proton collisions at a centre-of-mass energy of 7 TeV. The LHCb detector is a forward spectrometer described in Ref. [2].

The b-hadron lifetimes are extracted from a maximum likelihood fit to the proper time distributions of the fully reconstructed candidates. In order to avoid as much as possible a proper time dependent efficiency both the trigger and the offline selection are chosen to be lifetime unbiased: the selections avoid cutting on variables that are correlated with the b-hadron proper time, such as impact parameters of final state particles with respect to the primary vertex. The consequence of this strategy is that a very high level of prompt background will be kept in the $t \sim 0$ region, dominated by combinations of tracks originating from the primary vertex. Fortunately, the dominance of background in the prompt region does not cause problems for extraction of either lifetimes or CP

asymmetries, since the high proper time region is made very clean and provides most of the sensitivity to the physics parameters. The prompt combinatorial background is exploited to calibrate the proper time resolution directly from the data.

The analysis uses events accepted by a proper time unbiased $J/\psi \to \mu^+\mu^-$ trigger which collects pairs of tracks with opposite charge, identified as muons in the muon detector, with a minimum $p_{\rm T}$ of 500 MeV/c for each track and an invariant mass of the pair compatible with the known J/ψ mass. The offline selection imposes additional cuts on the vertex quality and impact parameter of the b-hadron, particle identification of kaons or protons in the final state using information provided by the RICH detectors, and a rather tight requirement of $p_{\rm T} > 1$ GeV/c on the 'bachelor' (K^+, K^{*0}, ϕ, Λ, $K^0_{\rm S}$) particle associated with the J/ψ. For the final states with a V^0 particle (Λ or $K^0_{\rm S}$) , an additional requirement of $L/\sigma_L > 5$ is made on the V^0, where L is the distance between the V^0 decay vertex and the b-hadron decay vertex and σ_L is the uncertainty of L.

3 Extracting the lifetime

The b-hadron lifetimes (τ) are extracted from a two-dimensional unbinned maximum likelihood fit to the distributions of the reconstructed b-hadron mass and proper time (t). The b-hadron mass is calculated with the J/ψ mass constrained to the PDG value. The signal mass distribution is modeled with a single Gaussian with floating mean and width. The distribution of the reconstructed mass of the background is modeled with a linear function, while alternative models are used to estimate the systematic uncertainty.

The signal proper time distribution is modeled with a single-sided exponential function multiplied by an acceptance function:

$$\mathcal{P}_{sig}(t) \;=\; Acc(t) \;\times\; \frac{1}{\tau}\, e^{-t/\tau} \qquad (t \geq 0)\,. \tag{1}$$

The acceptance function takes into account a small linear drop in the efficiency for large proper times. This acceptance is extracted from simulated events. A systematic uncertainty is assigned to account for potential data-simulation differences which is discussed in Section 5.

Note that due to the non-zero difference in the width of the B_s mass eigenstates, the proper time distribution of $B^0_s \to J/\psi\phi$ is not purely exponential, but rather the sum of two exponentials. In the analysis presented here we ignore this effect. The resulting measurement of the lifetime is denoted by $\tau^{\rm single}_{B^0_s}$ and essentially represents the mean value of the theoretical proper time distribution in $B^0_s \to J/\psi\phi$ decays. The extraction of $\Delta\Gamma_s$ from an angular analysis will be reported elsewhere.

The proper time distribution for background events is modeled by the sum of three contributions with different "lifetimes":

$$\mathcal{P}_{bkg}(t) = f_1\,\frac{e^{-t/\tau_1}}{\tau_1} \;+\; f_2\,\frac{e^{-t/\tau_2}}{\tau_2} \;+\; (1-f_1-f_2)\,\delta(t) \qquad (t \geq 0) \tag{2}$$

where $\delta(t)$ is a delta function with zero mean, which models the purely prompt combinatorial background, and f_i are the fractions of the two long-lived components.

Signal and background proper time models are convoluted with a resolution function that is the sum of three Gaussian components with different widths (σ_i) but a common mean (μ):

$$R(t,t') \;\propto\; \sum a_i \frac{1}{\sqrt{2\pi}\sigma_i} \exp\left[-\frac{(t-t'-\mu)^2}{2\sigma_i^2}\right] . \tag{3}$$

The a_i's are the fractions of the different Gaussian components. The parameters of the resolution model are extracted from a fit that includes the prompt combinatorial background. This means that they are essentially determined by the contribution of events with negative reconstructed proper times.

4 Results

Figures 1 to 5 show projections of the fitted function on the reconstructed b-hadron proper time and mass for the fit in the wide proper time range $t \in [-2, 14]$ ps. The mass range used for the fit is different for each exclusive mode and is described in the corresponding figure caption. Note that the background in the invariant mass projections is dominated by events with small reconstructed proper time. Comparison of the fitted function to the data at negative proper time shows that the resolution model is not perfect. Fits are performed using alternative resolution models in order to estimate the systematic uncertainties due to insufficient knowledge of the resolution model.

In order not to bias the result by a non-perfect modeling of the prompt background, the b-hadron lifetimes are extracted from fits to candidates with reconstructed proper times $t > 0.3$ ps only. The contribution from background events in this proper time range is so small that a non-perfect background model has only little effect on the fitted lifetimes. In these fits the prompt background component is removed from the background proper time model. The parameters of the long-lived components are floated. However, the parameters of the resolution function are fixed to those obtained from the fit to the wide proper time range $t \in [-2, 14]$ ps.

The reconstructed mass and proper time projections of these fits are shown in Figs. 6 to 10. The extracted lifetimes and the signal yields in the proper time range $t \in [0.3, 14]$ ps, taken as our default results, are shown in Table 2. The uncertainties are statistical only.

Channel	Lifetime (ps)	Yield
$B^+ \to J/\psi K^+$	1.689 ± 0.022	6741 ± 85
$B^0 \to J/\psi K^{*0}$	1.512 ± 0.032	2668 ± 58
$B^0 \to J/\psi K^0_{\rm S}$	1.558 ± 0.056	838 ± 31
$B^0_s \to J/\psi \phi$	1.447 ± 0.064	570 ± 24
$\Lambda_b \to J/\psi \Lambda$	1.353 ± 0.108	187 ± 16

Table 2: Signal event yields and lifetimes extracted from the likelihood fits to the candidates with proper time $t \in [0.3,\, 14]$ ps.

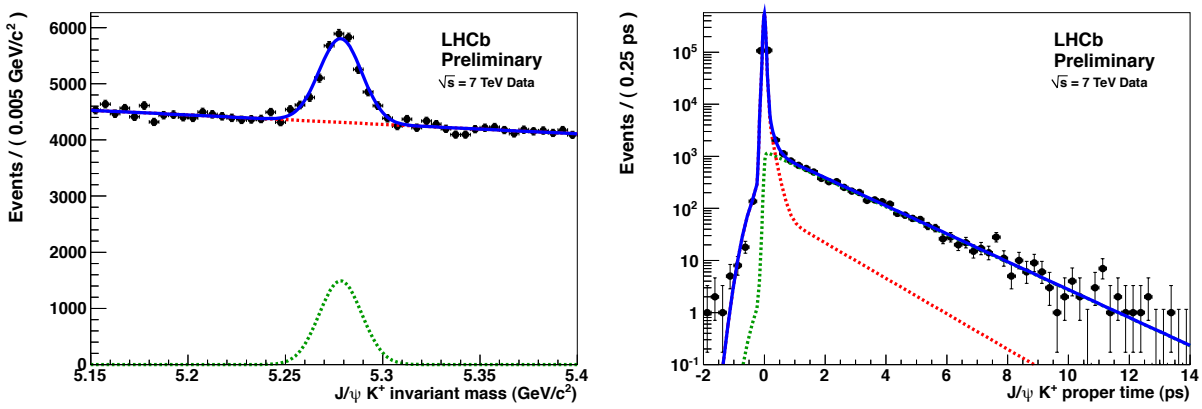

Figure 1: B^+ mass (left) and proper time (right) projections of the two-dimensional fit to the $B^+ \to J/\psi K^+$ candidates. The total fit is represented by the blue solid line, the signal contribution by the green dashed line and the background contribution by the red dashed line. The mass range for the fit is $m \in [5.15, 5.40]$ GeV/c^2.

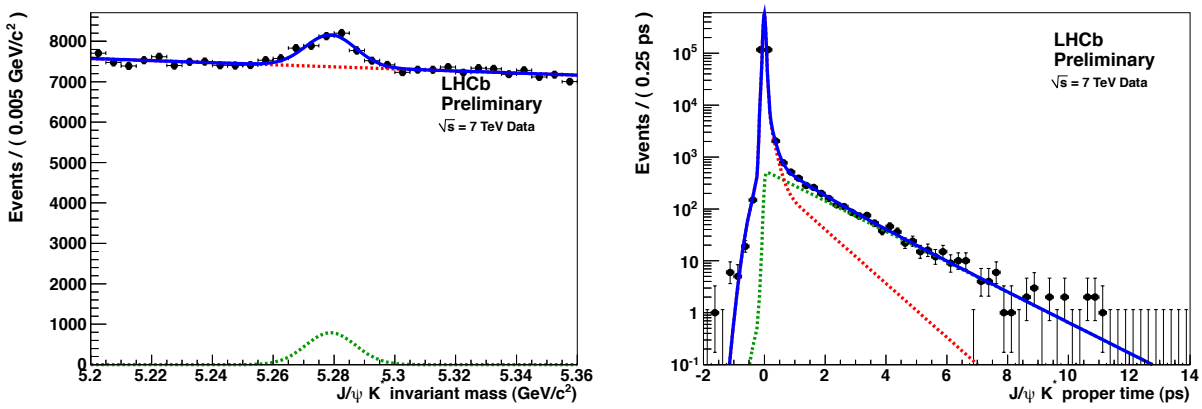

Figure 2: B^0 mass (left) and proper time (right) projections of the two-dimensional fit to the $B^0 \to J/\psi K^{*0}$ candidates. The total fit is represented by the blue solid line, the signal contribution by the green dashed line and the background contribution by the red dashed line. The mass range for the fit is $m \in [5.20, 5.36]$ GeV/c^2.

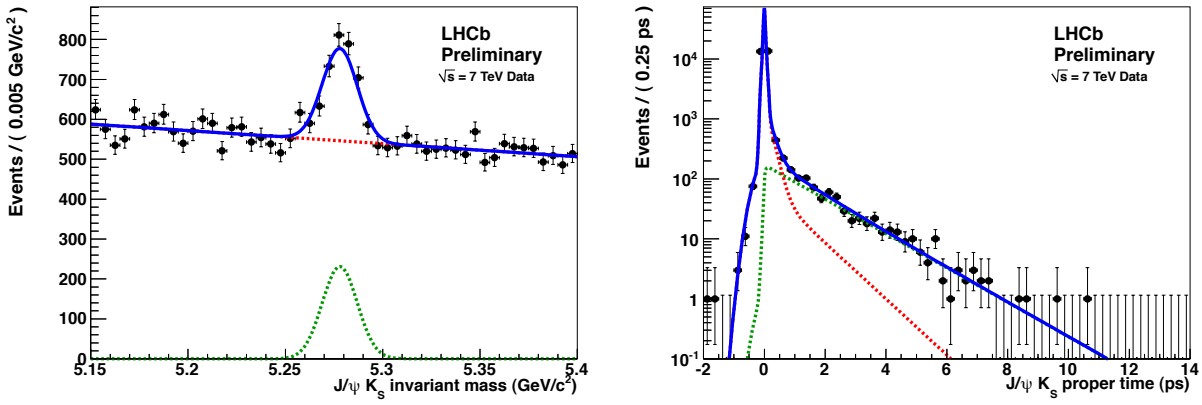

Figure 3: B^0 mass (left) and proper time (right) projections of the two-dimensional fit to the $B^0 \to J/\psi K^0_S$ candidates. The total fit is represented by the blue solid line, the signal contribution by the green dashed line and the background contribution by the red dashed line. The mass range for the fit is $m \in [5.15, 5.40]$ GeV/c^2.

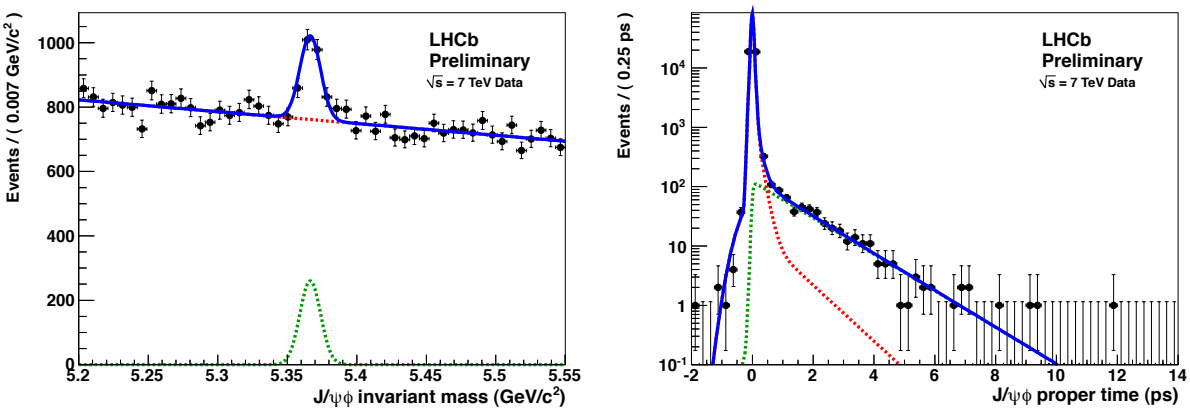

Figure 4: B_s^0 mass (left) and proper time (right) projections of the two-dimensional fit to the $B_s^0 \to J/\psi\phi$ candidates. The total fit is represented by the blue solid line, the signal contribution by the green dashed line and the background contribution by the red dashed line. The mass range for the fit is $m \in [5.20, 5.55]$ GeV/c^2.

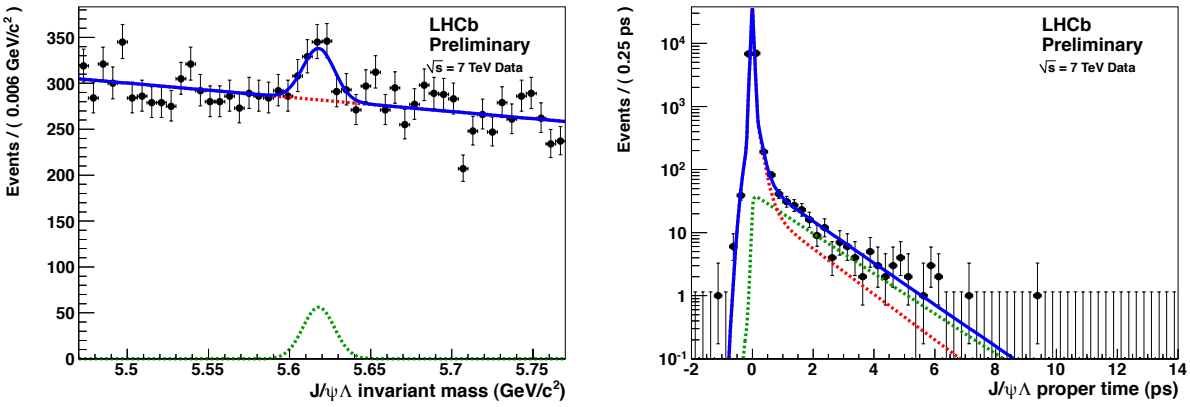

Figure 5: Λ_b mass (left) and proper time (right) projections of the two-dimensional fit to the $\Lambda_b \to J/\psi\Lambda$ candidates. The total fit is represented by the blue solid line, the signal contribution by the green dashed line and the background contribution by the red dashed line. The mass range for the fit is $m \in [5.47, 5.77]$ GeV/c^2.

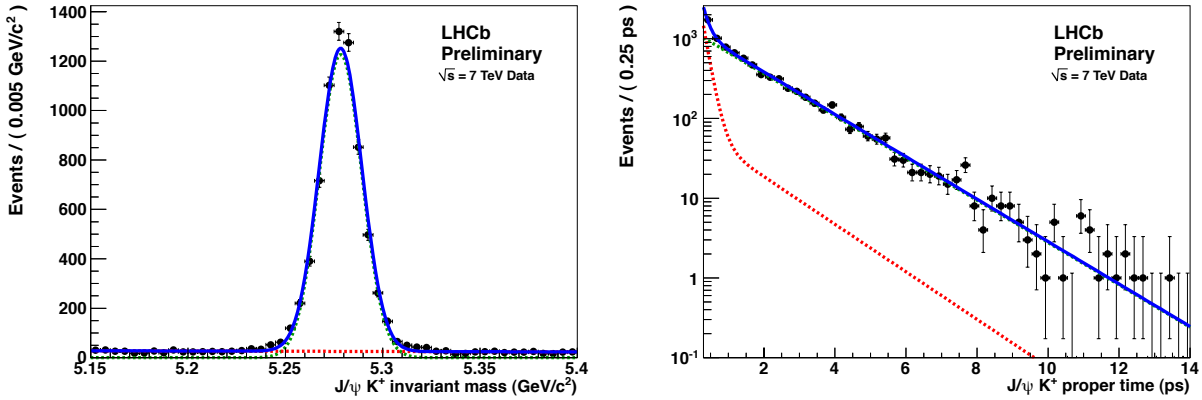

Figure 6: B^+ mass (left) and proper time (right) projections of the two-dimensional fit to the $B^+ \to J/\psi K^+$ candidates with $t > 0.3\,\text{ps}$. The total fit is represented by the blue solid line, the signal contribution by the green dashed line and the background contribution by the red dashed line. The mass range for the fit is $m \in [5.15, 5.40]$ GeV/c^2.

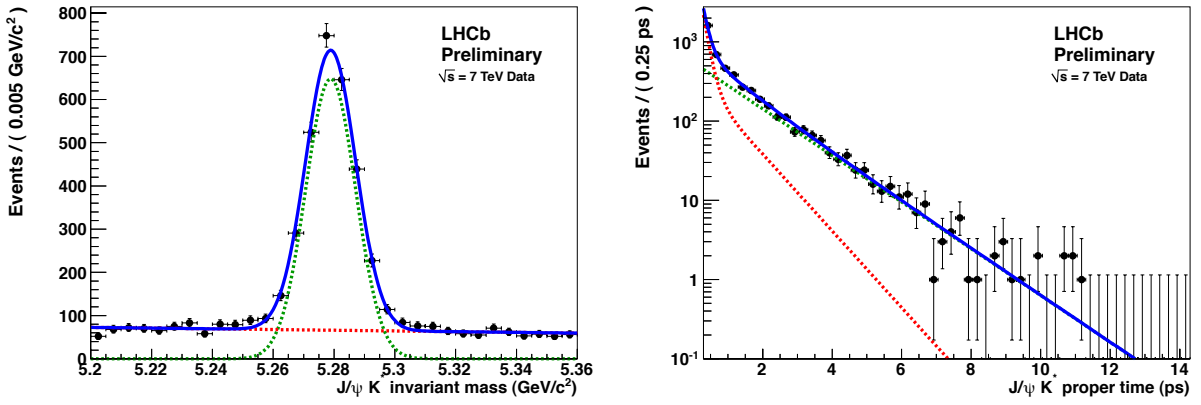

Figure 7: B^0 mass (left) and proper time (right) projections of the two-dimensional fit to the $B^0 \to J/\psi K^{*0}$ candidates with $t > 0.3\,\text{ps}$. The total fit is represented by the blue solid line, the signal contribution by the green dashed line and the background contribution by the red dashed line. The mass range for the fit is $m \in [5.20, 5.36]$ GeV/c^2.

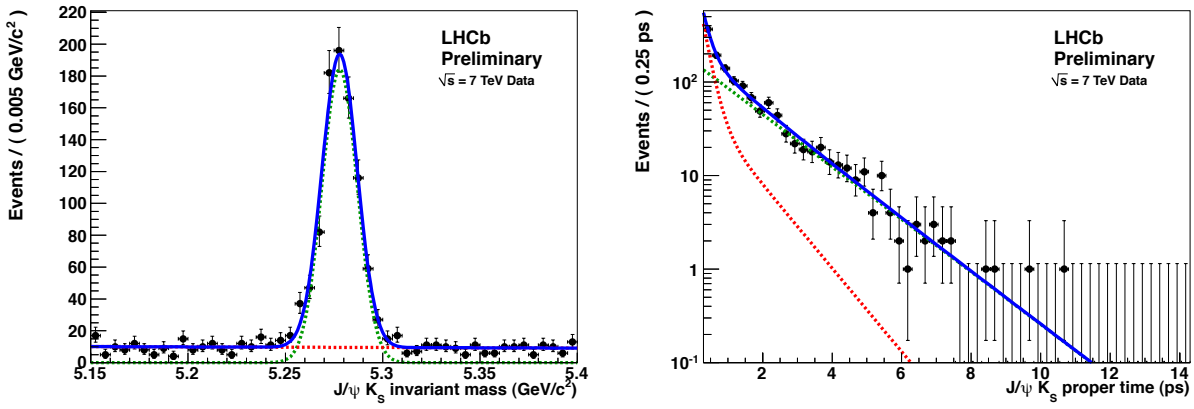

Figure 8: B^0 mass (left) and proper time (right) projections of the two-dimensional fit to the $B^0 \to J/\psi K^0_{\rm S}$ candidates with $t > 0.3\,$ps. The total fit is represented by the blue solid line, the signal contribution by the green dashed line and the background contribution by the red dashed line. The mass range for the fit is $m \in [5.15, 5.40]$ GeV/c^2.

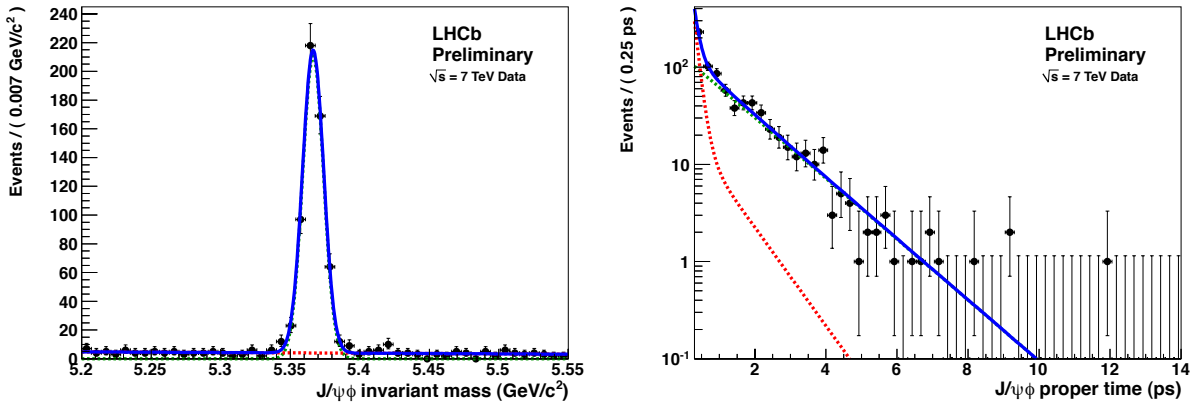

Figure 9: B^0_s mass (left) and proper time (right) projections of the two-dimensional fit to the $B^0_s \to J/\psi\phi$ candidates with $t > 0.3\,$ps. The total fit is represented by the blue solid line, the signal contribution by the green dashed line and the background contribution by the red dashed line. The mass range for the fit is $m \in [5.20, 5.55]$ GeV/c^2.

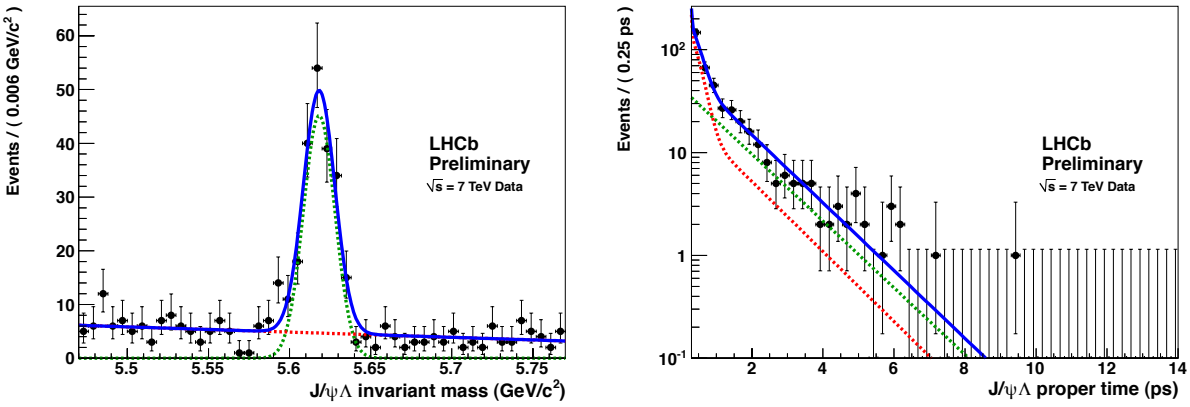

Figure 10: Λ_b mass (left) and proper time (right) projections of the two-dimensional fit to the $\Lambda_b \to J/\psi\Lambda$ candidates with $t > 0.3\,\text{ps}$. The total fit is represented by the blue solid line, the signal contribution by the green dashed line and the background contribution by the red dashed line. The mass range for the fit is $m \in [5.47, 5.77]$ GeV/c^2.

5 Systematic uncertainties

We consider several sources of systematic uncertainties, summarized in Table 3. Contributions from non-perfect modeling of signal and background in the likelihood fits are estimated by rerunning the fits with alternative parameterizations. Such estimates are inherently sensitive to statistical fluctuation and we expect the uncertainties to go down with more statistics.

As explained above the proper time acceptance is a function of the proper time describing a drop in reconstruction efficiency for large proper time. Currently, this acceptance is extracted from fully-simulated events. The full acceptance correction is applied in the likelihood fit used to extract the b-hadron lifetime. The systematic uncertainty associated with the modeling of the proper time distribution of the signal is conservatively estimated to be the difference between the results with and without the acceptance correction. This is currently the dominating systematic uncertainty in this analysis.

Uncertainties related to the momentum scale are estimated from the measured invariant mass of known resonances, most notably charmonium and b-hadrons. The uncertainty in the decay length scale is estimated from a comparison of survey alignment with alignment extracted from reconstructed tracks. Both the momentum scale uncertainty and the decay length scale uncertainty are expected to improve with a better understanding of the alignment of the tracking detectors.

	$B^+ \to J/\psi K^+$	$B^0 \to J/\psi K^{*0}$	$B_s^0 \to J/\psi \phi$	$B^0 \to J/\psi K_S^0$	$\Lambda_b \to J/\psi \Lambda$
signal mass model	0.002	0.002	0.010	0.014	0.012
signal time model	0.043	0.038	0.040	0.015	0.022
bkg. mass model	0.009	0.020	0.005	0.008	0.023
bkg. time model	0.003	0.006	0.003	0.006	0.006
time resol. model	0.005	0.005	0.005	0.005	0.005
momentum scale	0.001	0.001	0.001	0.001	0.001
decay length scale	0.001	0.001	0.001	0.001	0.001
quadratic sum	0.047	0.042	0.056	0.022	0.035

Table 3: Systematic uncertainties in the lifetime measurements (ps).

6 Conclusions

Using a sample of approximately $36\,\mathrm{pb}^{-1}$ collected with the LHCb detector in 2010 at a centre-of-mass energy of 7 TeV, we extract the main b-hadron lifetimes in the exclusive final states $B^+ \to J/\psi K^+$, $B^0 \to J/\psi K^{*0}$, $B_s^0 \to J/\psi\phi$, $B^0 \to J/\psi K_{\rm S}^0$ and $\Lambda_b \to J/\psi\Lambda$ with $J/\psi \to \mu^+\mu^-$. The trigger and offline event selections have been optimized to reduce the effect of a possible lifetime bias.

The results extracted from a two-dimensional unbinned maximum likelihood fit to the reconstructed b-hadron candidate invariant mass and proper time distributions are

$$\begin{aligned}
\tau(B^+ \to J/\psi K^+) &= 1.689 \pm 0.022 \pm 0.047\ \mathrm{ps}\,, \\
\tau(B^0 \to J/\psi K^{*0}) &= 1.512 \pm 0.032 \pm 0.042\ \mathrm{ps}\,, \\
\tau(B^0 \to J/\psi K_{\rm S}^0) &= 1.558 \pm 0.056 \pm 0.022\ \mathrm{ps}\,, \\
\tau^{\rm single}(B_s^0 \to J/\psi\phi) &= 1.447 \pm 0.064 \pm 0.056\ \mathrm{ps}\,, \\
\tau(\Lambda_b \to J/\psi\Lambda) &= 1.353 \pm 0.108 \pm 0.035\ \mathrm{ps}\,.
\end{aligned}$$

where $\tau^{\rm single}(B_s^0 \to J/\psi\phi)$ is the lifetime measured with $B_s^0 \to J/\psi\phi$ using a single exponential to model the proper time distribution, i.e., ignoring the non-zero decay-width difference of the B_s^0 system.

The systematic uncertainties are dominated by our imperfect knowledge of the dependence of the event reconstruction efficiency on proper time. We are currently using simulation to more precisely determine the acceptance effects arising from different steps of the event reconstruction and pin down their exact origins. Efforts are also being made to improve agreement between data and simulation. We are confident that this uncertainty can be largely reduced in the future.

Our measurements are in agreement with the world averages, but not yet competitive. We expect that with more data collected in the course of 2011, LHCb will significantly improve the accuracy of these measurements.

References

[1] K. Nakamura *et al.* (Particle Data Group), "Review of particle physics", J. Phys. G 37, 075021 (2010).

[2] The LHCb collaboration, "The LHCb detector at LHC", Journal of Instrumentation (JINST) 3 (2008) S08005.

[3] T. Sjöstrand, S. Mrenna and P. Skands, "PYTHIA 6.4: Physics and manual", hep-ph/0603175, JHEP 05 (2006) 026.